

Radon Transform, Projections, Fourier Slice Theorem, Backprojection Methods, and Relation to SAR

September 21, 2015

1 Preliminaries

Definition 1 (Fourier transform). Let $f \in L_p(\mathbb{R}^2)$. The Fourier transform $F : L_p \rightarrow L_q$, of f , denoted \hat{f} at (ω_1, ω_2) is defined by

$$\hat{f}(\omega_1, \omega_2) = \int_{\mathbb{R}^2} f(x, y) e^{-i2\pi(x, y) \cdot (\omega_1, \omega_2)} dx dy. \quad (1)$$

For the remainder of this document, given an angle θ , we will let ξ_θ denote the unit vector $(\cos \theta, \sin \theta)$.

Definition 2 (Radon Transform). Let $f \in L_2(\mathbb{R}^2)$. The Radon transform of f at (t, θ) , denoted $Rf(t, \theta)$ is given by

$$Rf(t, \theta) = \int_{\mathbb{R}^2} f(x, y) \delta(t - (x, y) \cdot \xi_\theta) dx dy. \quad (2)$$

Equivalently,

$$Rf(t, \theta) = \int_{t=(x, y) \cdot \xi_\theta} f(x, y) d\sigma \quad (3)$$

2 Tomography

In many applications, the Radon transform of a function f will be acquired at a dense set of points t , for some small number of angles θ . Therefore it is sometimes convenient to consider the Radon transform as a collection of projections of f at angles $\{\theta_i\}_{i=1}^k$. We define the projection operator at angle θ by

$$P_\theta f(x) = \int_{\mathbb{R}} f((x, y) Q_\theta^T) dy, \quad (4)$$

where

$$Q_\theta = \begin{pmatrix} \cos \theta & -\sin \theta \\ \sin \theta & \cos \theta \end{pmatrix},$$

is a rotation matrix. Note that $Rf(x, \theta) = P_\theta f(x)$.

The general tomography problem refers to reconstructing an approximation of f given a collection of projections of f , $\{P_{\theta_i} f\}_{i=1}^k$. Typical difficulties include, limited angular ranges (like in SAR), few projections due to object sensitivity, and noisy data. At the very least, it should be verified that f can be exactly recovered from full knowledge of $P_\theta f(x)$ at all values $\theta \in [0, \pi)$ and $x \in \mathbb{R}$. The following theorem confirms this:

Theorem 3 (Fourier Slice Theorem). $\widehat{P_\theta f}(\omega) = \hat{f}(\omega \xi_\theta)$, *i.e.*

$$\int_{\mathbb{R}} P_\theta f(x) e^{-i2\pi x \omega} dx = \iint_{\mathbb{R}^2} f(x, y) e^{-i2\pi \omega (x, y) \cdot \xi_\theta} dx dy. \quad (5)$$

Proof. Simply write out the expression for $\widehat{P_\theta f}(\omega)$ as a double integral, and make the substitution $(\alpha, \beta) = (x, y)Q_\theta^T$. \square

The Fourier slice theorem gives rise to particular reconstruction techniques known as Fourier backprojection, which is basically an inversion formula that compensates for the polar sampling of f that leaves larger spacing for high frequencies (demonstrated in figure-1). This compensation is done by applying a ramp filter to the Fourier samples which gives more weight to the high frequencies.

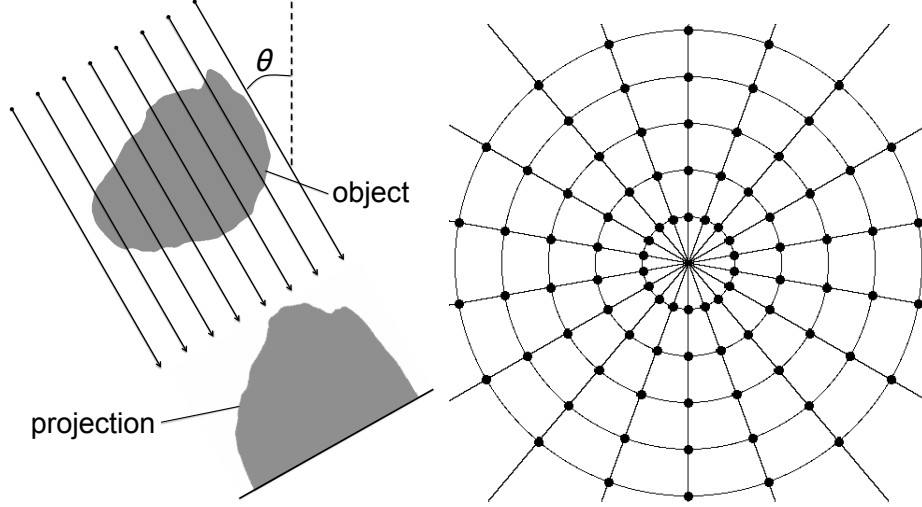


Figure 1: Left: a projection of a blob at angle θ . Right: Visual representation of location of polar samples in Fourier space equivalent to a set of angular projections.

3 Practical Tomography Setting

Given data: $\{P_{\theta_\ell} f(x_p)\}_{\ell=1, p=1}^{k, \alpha}$ ($k = 50$ and $\alpha = 1024$ for instance).

Goal: Reconstruct a pixel image $f_{rec} = \{f_j\}_{j=1}^{n^2}$, which is a “good” approximation of the object.

Each integral can be modeled as a weighted sum of f (like a Riemann sum):

$$P_{\theta_\ell} f(x_p) = \sum_{j=1}^{n^2} w_j^{\ell, p} f_j = \langle w^{\ell, p}, f \rangle.$$

We define $b_{m(\ell, p)} = P_{\theta_\ell} f(x_p)$,

$$W = \{w_j^{\ell, p}\}_{j, \ell, p=1}^{n^2, k, \alpha} \quad \text{and} \quad b = \{b_{m(\ell, p)}\}_{m=1}^{k \cdot \alpha},$$

where for W , the index j is over the columns and ℓ, p is over the rows and $W \in \mathbb{R}^{(k \cdot \alpha) \times n^2}$.

Note that for each (ℓ, p) , $\#\{j : w_j^{\ell, p} \neq 0\} = O(n)$, so that W is relatively sparse. Finally then, the reconstruction is given by

$$f_{rec} = \arg \min_f \left\{ \|Wf - b\|_2^2 + \lambda \|f\|_N \right\}, \quad (6)$$

or

$$f_{rec} = \arg \min \|f\|_N \quad \text{s.t.} \quad Wf = b, \quad (7)$$

where $\|\cdot\|_N$ is some norm or seminorm.

Typically, the number of measurements $k \cdot \alpha \ll n^2$ so that the linear system is underdetermined. However, this can be misleading, since the rows of W are not necessarily linear independent. Also, likely W does not satisfy the incoherency properties or RIP properties needed for the compressed sensing theories, although some have argued otherwise via the Fourier Slice Theorem.

3.1 Real Space Backprojection Methods

Backprojection methods for tomographic reconstruction are geometrically motivated and simply iteratively “smear” back the projection values onto the image domain. The most basic of these is known as algebraic reconstruction technique (ART) and was discovered in tomography (1970). The method was independently discovered in linear algebra and is known Kaczmarz method (1937).

ART/ Kaczmarz: Let the the current solution at iterate k be f^k . At iterate $k + 1$ randomly select a projection value $b_{m(\ell,p)}$ and smear the difference between f^k and b_m evenly over f^k to obtain f^{k+1} satisfying

$$\langle f^{k+1}, w^{\ell,p} \rangle = b_{m(\ell,p)}. \quad (8)$$

This yields the formula

$$f^{k+1} = f^k + \lambda_k \frac{b_m - \langle w^{\ell,p}, f^k \rangle}{\|w^{\ell,p}\|_2^2} w^{\ell,p}. \quad (9)$$

Generalization (SIRT, SART): One can generalize the method of ART so that projection values $\{b_{m(\ell,p)}\}$ are “simultaneously” backprojected at each iterate. This yields techniques such as simultaneous iterative reconstruction technique (SIRT). This is possible for example, one can imagine that projection values $\{b_{m(\ell,p)}\}_p$ for a fixed angle θ_ℓ correspond to parallel paths through the image and therefore do not interfere with each other for the backprojection procedures.

Convergence: Backprojection methods are known to converge to the least squares solution. That is, in terms of (7), the norm is $\|\cdot\|_2$, and the solution is given by

$$f_{rec} = W^+ b = W(WW^T)^{-1} b. \quad (10)$$

Therefore one can use alternative methods such as conjugate gradient least square (CGLS). However, CGLS methods do not handle additional constraints well, such as $f \geq 0$ and volume constraints, where as SIRT can naturally implement these conditions.

Parseval’s theorem (and orthogonality) gives us

$$\|f\|_2 = \|\hat{f}\|_2. \quad (11)$$

Therefore returning to the Fourier slice theorem, all values (ω_1, ω_2) of $\widehat{f_{rec}}(\omega_1, \omega_2)$ given by a least squares solution will be zero over the lines in which the data is missing. This is obviously not an ideal solution.

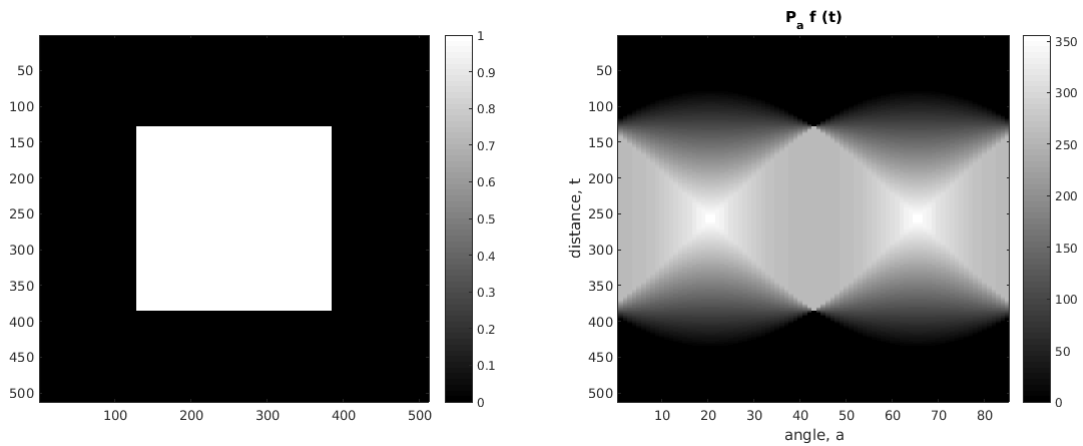


Figure 2: Simple box image (left) and the projections of the box (right) viewed as a sinogram.

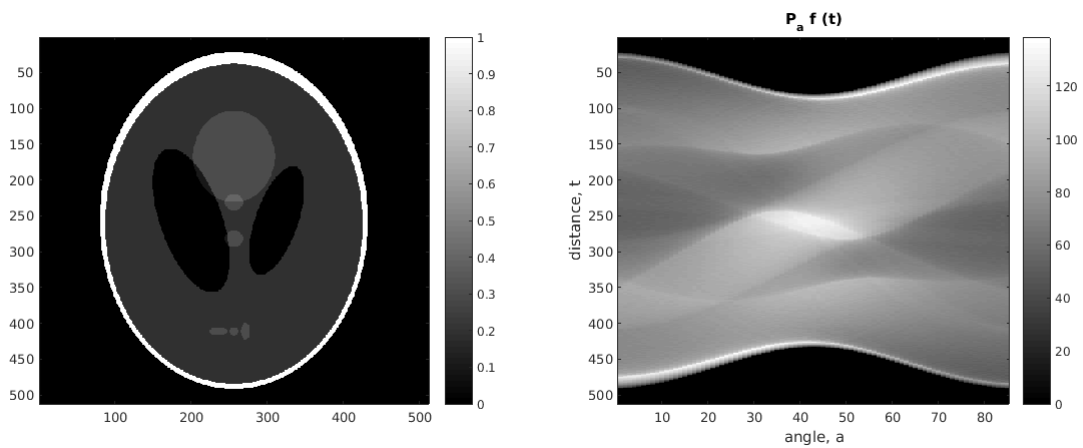


Figure 3: Logan-shepp phantom (left) and the projections of the phantom (right) viewed as a sinogram.

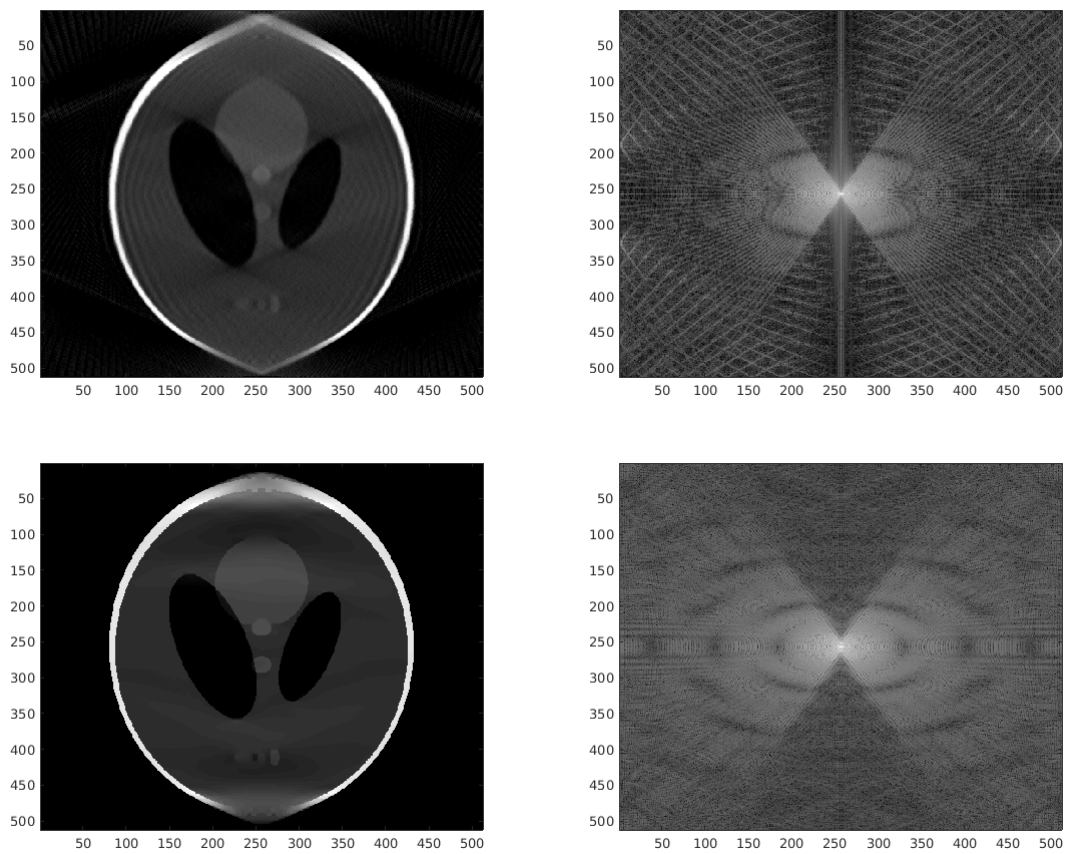


Figure 4: Reconstructions from a total angular range of 120 degrees out of 180. Top: Backprojection/ least squares. Bottom: TV regularized reconstruction. On the left are the reconstructions and the right are log scale images the Fourier transform of the reconstructions.

4 Relation to SAR Data (Briefly)

With data acquisition for SAR, a plane sends pulses of electromagnetic waves to the scanning field of interest as it flies along some path, which is perhaps circular. The echo or response is measured by an antenna for each positioning of the plane relative to the scanning field. The information gathered is equivalent to values of the Fourier transform of a reflexivity map of the scanning field, along polar lines where the angle of each line corresponds to position of the plane relative to the scanning field. Certainly, all of this is discretized, with a discrete number of angles and values acquired for each angle. For example, we may have $\{\hat{f}(\omega_j \xi_{\theta_i})\}_{i,j=1}^{k,n}$. Certainly then, by previous discussion the SAR data is equivalent to tomography data simply by a one-dimensional Fourier transforms and backprojection techniques are similar in this setting.